# Analytical Study for the selection of mask size and shape for the machining of circular features

WCMNM 2020

Gaganpreet Singh[1], Bhawandeep Sharma[1], J. Ramkumar[1], S.A. Ramakrishna[2,3]

[1] *Department of Mechanical Engineering, IIT Kanpur, Kanpur - 208016*
[2] *Department of Physics, IIT Kanpur, Kanpur - 208016*
[3] *Director, Central Scientific Instruments Organisation, Chandigarh - 160030*

**Abstract**

In this article, we had analytically studied the effect of the shape and size of the mask on the machining quality of the circular feature. Machining quality was measured in the form of unmachined area '$A_n$' that will be left after machining a specific area, in the minimum machining time '$T_m$.' For this study, we have considered square and circular spot size (spot size is 1/10 of the mask size) of varying size, i.e., from 1 mm to 10 mm and for each case, the overlap was also varied from 0.1 to 0.9. From the analytical solution, we found that the square spot is better than the circular spot for minimum machining time for given spot size, whereas for minimum unmachined area circular spot is better than the square spot. This study could be useful in the industrial-scale manufacturing of circular features using the mask projection technique in laser machining.

**Keywords:** Mask Projection Technique, Circular machining, large area machining, mask size and shape

## 1. Introduction

High feature resolution, high speed of processing, the low unit cost of manufacturing, production of novel geometries, and rapid prototyping capabilities are vital in the evolution of many industrial sectors such as microelectronics, aerospace semiconductor, and biotechnology which are evolving rapidly. These needs have been met by pulsed laser micro-processing techniques [1–3].

Laser machining can be done by two means, i.e., raster scanning and mask projection technique [4]. In raster scanning or laser writing technique, laser beam profile remains constant, whereas the size is dependent on the numerical aperture of the lens used for focusing, while in mask projection technique, the laser beam profile can be changed as desired. Mask projection technique has lots of advantages such as the mask is remote from the machining and hence does not suffer from debris damage, the use of a de-magnifying projection lens allows easy manufacturing of the mask and also lower fluence at the mask plane, hence, prolonging the mask lifetime. The remoteness of the mask from the workpiece allows independent motion of the mask, therefore, multiple patterns can be superimposed on the sample by changing the masks. Over the years, researchers have shown the methodologies by which complicated structures can be fabricated using mask projection techniques such as photomask [5], contour mask scanning [6] and planetary mask contour scanning method [7].

Using the contour mask and workpiece scanning method Nadeem et al. [8] had fabricated a microlens array using the excimer laser. The same researcher had also studied the effect of the spot overlap on the channels' roughness at an oblique angle. They concluded that with an increase in the overlap, the roughness decreases. However, they did not study the effect of mask shape on the roughness. Such a study is required because, with an increase in the overlap, there is also an increase in the machining time '$T_m$', which is an essential factor while machining of a large area. Such a study is also required for machining of circular features, because designs for various applications such as metamaterial microwave absorbers and lens arrays have circular features. Such products demands high production rates while maintaining the quality of the features.

In this study, we had analytically studied the effect of the spot shape and size (which is 1/10 of the mask size) and overlap on the machined area and machining time for the machining of a circular feature. This study not only will helps the industries to reduce the machining time, but also to improve the quality of their product. Hence, it will improve the productivity of manufacturing unit without any additional cost.

## 2. Methodology

In any arbitrary design which needed to be machined by laser using mask projection technique, it can be divided into three basic geometries shapes, i.e. straight lines, inclined lines, and circles. Machining straight features is a more straightforward process as compare to circular features. Machining circular features lead to the unmachined area '$A_n$', which can be defined as the area that was supposed to be machined but remained unmachined since laser pulse does not interact with that portion,. The '$A_n$' will lead to the generation of roughness at the edges hence decreases the machining quality. In this study, we had considered machining of the circular features with various spot sizes and shapes. As shown in equation 1, spot size plays a significant role in deciding the machining time '$T_m$'. Therefore, different spot sizes and shapes for machining circular features were compared based on two parameters, '$T_m$' and '$A_n$'. The machining time '$T_m$' is the total time needed to machine the required feature and is calculated using equation 2 [10].

$$Scanning\ Speed = \frac{f \times spot\ size \times (1-O)}{No.\ of\ pulses\ at\ the\ spot} \quad (1)$$

$$T_m = \frac{Machined\ Length}{Scanning\ Speed} \quad (2)$$

where '*f*' is the repetition rate, '*spot size*' is the area under machining when the sample is not moving and '*O*' is the overlap which can be defined as the non-dimensional number which shows the fraction/percentage of the successive pulse that will fall on the area which was already machined by the previous pulse. We had studied the machining of circular feature which are sequentially discussed as following:

*2.1. Machining of a circular feature with a square spot*

Fig. 2 shows the schematic of the machining of a circular feature using a square spot, where '*R*' is the radius of the circular feature to be machined and '*m*' is half of the spot size. For all the cases, '*spot size*' was varied from 0.1 mm to 1 mm with a step size of 0.1 mm and overlap from 0.1 to 0.9 with a step size of 0.01. For calculation, constant repetition rate ('*f*') and the number of pulses at the spot were considered, which are 5 Hz and 10, respectively. Also, '*R*' was considered equals to 7 mm, and it was assumed that '*R*' is much greater than '*m*' (i.e. *R*>>*m*). For '$T_m$' the total machining length was considered as the total distance moved by the spot to cover the perimeter of a circle having radius '*R*'. Equation 7 and 8 shows the derived formulas for '$A_n$' and '$T_m$'.

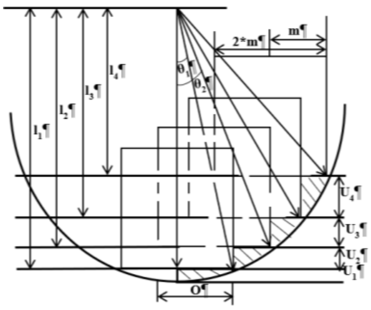

Fig 2: Schematic of machining of circle using square spot

$$Sin(\theta_n) = \frac{m + 2 \times (n-1) \times m(1-O)}{R} \tag{3}$$

$$l_n = \frac{m \times (1 + 2 \times (n-1) \times (1-O))}{\tan(\theta_n)} \tag{4}$$

$$U_1 = R - L_1 \tag{5}$$

$$U_n = R - l_n - \textstyle\sum_{i=1}^{n-1} U_i \quad \text{(for } n \geq 2\text{)} \tag{6}$$

$$A_n = \frac{m}{2}\left(\textstyle\sum_{i=1}^{n} U_i - O \times \left(\sum_{j=2}^{n} U_j\right)\right) \tag{7}$$

$$T_m = \frac{m \times (1 + 2 \times (n-1) \times (1-O))}{Scanning\ Speed} \tag{8}$$

where '$\theta_n$' is the angle between the center of the machining spot at the start of the machining and corner of the $n^{th}$ machined spot intersecting with the circle's boundary, the '$l_n$' is the distance between the center of the circle and the lower edge of the $n^{th}$ machining spot and '*n*' is the count of the machining spots from the start of machining.

Fig. 3 and 4 show the plot for the variation in the '$T_m$' and '$A_n$'. As shown in Figure 3, there is an increase in the machining time with a decrease in the spot size and increase of overlap. However, the other interesting observation is that different combinations of '*m*' and '*O*' give the same '$T_m$'. The same is also true for the case of '$A_n$'. Further, the turbulent nature of the change in the '$T_m$' and '$A_n$' shows that the current study becomes more critical as the machining features become complex. Taking the example of this case, we have discussed the importance of the obtained result in the next section.

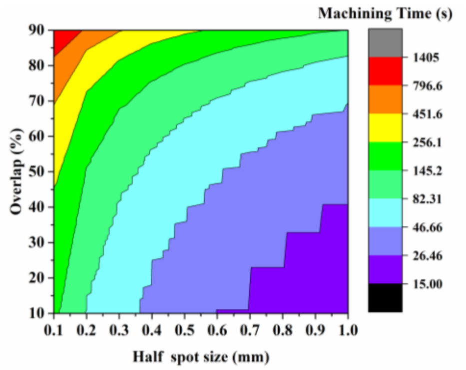


Fig 3: Variation of machining time with machining spot size and overlap for machining of the circle with a square spot

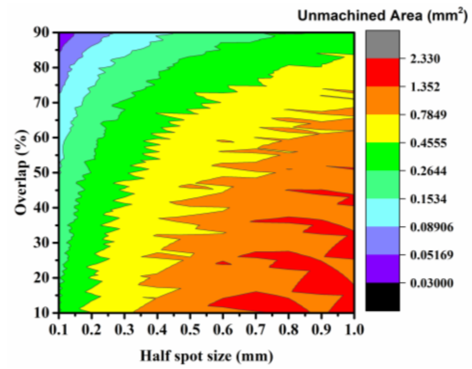


Fig 4: Variation of the unmachined area with machining spot size and overlap for machining of a circle with a square spot

*2.1. Machining of a circular feature with a circular spot*

Fig 5 shows the schematic of the machining of the circle with a circular spot. For the calculation of '$T_m$' and '$A_n$' in this case, two assumptions have been made which are: (a) the radius of circle '*R*' is much greater than '*m*' (i.e. *R*>>*m*) and (b) the arc length subtended by angle 'θ' (angle subtended by the lines joining center of two adjacent machining spot) is equivalent to a straight line of length $2 \times m \times (1 - O)$.

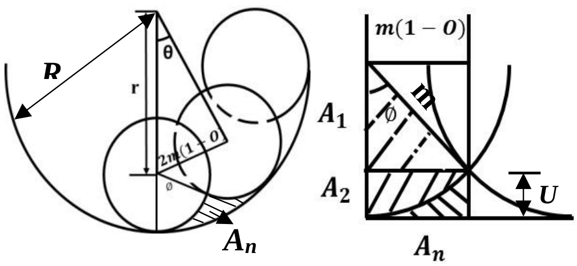


Fig. 5 Schematic of machining of the circle using a circular spot

Using the above mentioned approximation, the derived equations for '$A_n$' are as follow:

$$\Theta = \frac{2m \times (1-O)}{r} \quad (9)$$

$$U = m(1 - cos\emptyset) \quad (10)$$

$$A_1 = \frac{1}{2} \times mCos\emptyset \times m(1-O) \quad (11)$$

$$A_n = m(1-O) \times U - \frac{1}{2\pi} \times \pi m^2 \times \emptyset - A_1 \quad (12)$$

For '$T_m$' the total machining length was considered as total distance moved by the spot to cover the parameter of the circle Using the above equations, the plots for the '$T_m$' and '$A_n$' were plotted as shown in figure 6 and 7, respectively using '*R*' as 7 cm.

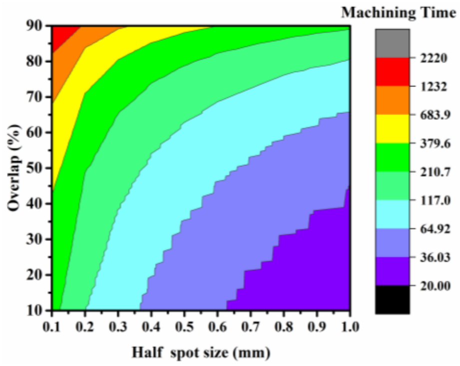


Figure 6: Variation of machining time with machining spot size and overlap for machining of a circle with a circular spot

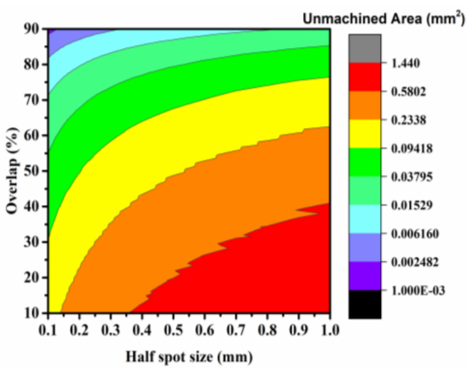


Figure7: Variation of an unmachined area with machining spot and overlap for machining of a circle with a circular spot

## 3. Result and Discussion

From the above-mentioned cases, it can be seen that the relation between machining time and unmachined area with the spot size and overlap is not always linear and same machining time and unmachined area can be obtained using different combination of spot size and overlap. To better understand the results obtained from the above study, we took the case of machining circular features using a square spot. '$T_m$' and '$A_n$', were calculated for a circle having radius of 7 mm by varying 'm' from 0.1 mm to 1 mm and 'O' from 0.1 to 0.9. We have then studied the variation in the '$T_m$' by fixing '$A_n$' as 1 mm$^2$, 0.8 mm$^2$ and 0.7 mm$^2$. As can be seen in fig 8, the same '$A_n$' can be achieved by using various combinations of '*m*' *and* '*O*' in all cases. However, the '$T_m$' varies as the combination of '*m*'; and '*O*' varies. This shows that we can select that combination that gives the minimum '$T_m$' (highlighted using a square box in all cases in fig. 8) for a fixed value of '$A_n$'.

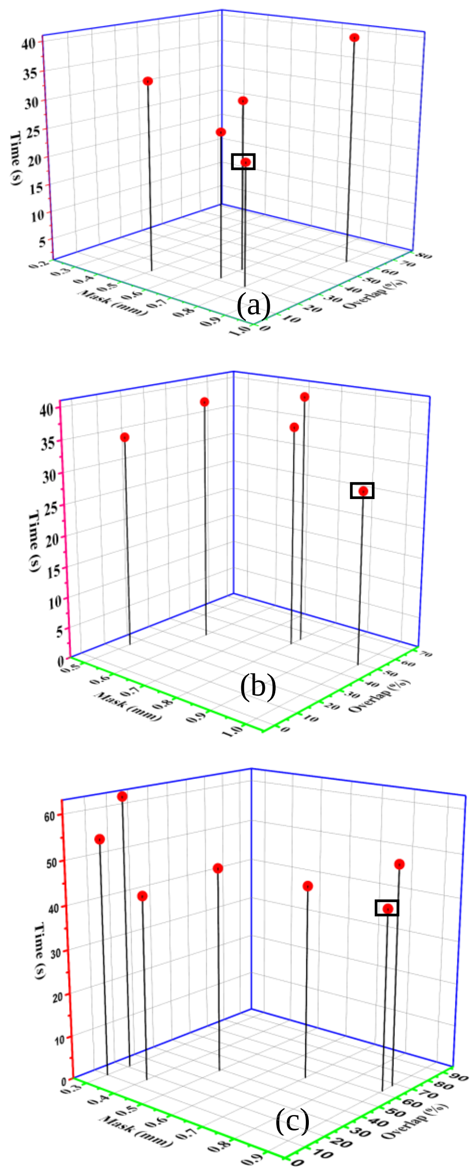


Fig 8: Variation of machining time for fixed unmachined area of (a) 1 mm$^2$ (b) 0.8 mm$^2$ and (c) 0.7 mm$^2$

Further, figures 9 and 10 show the comparison of '$A_n$' and '$T_m$' respectively for machining of a circle having radius 7 mm with a square and a circular spot of size 0.3 mm and 0.7 mm. As can be seen from fig 9, instead of following a straight path, '$A_n$' follows a zig-zag pattern with a decrease in '*O*'. Although zig-zag pattern is more evident in square spot cases, it is also present in circular spot cases with low amplitudes. It can be further seen that for all the values of '*O*' a circular machining spot have lesser '$A_n$' for the given '*m*'. This shows that a circular spot gives better machining quality than a square spot. Further, in fig 10, it can be seen that for given '*m*' and machining length '*L*', circular spot size takes more time for machining than the square spot. However, a circular spot of 0.7 mm gives lower '$A_n$' as compared to a square spot of 0.3 mm after 30% overlap but the '$T_m$' taken by the circular spot of 0.7 mm is always less than the '$T_m$' taken by 0.3 mm. These results show that circular spot size provides better machining quality compared to the square spot size along with the minimum '$T_m$'. Now, we can choose between machining quality and machining time as per our requirement by merely changing the spot shape and size.

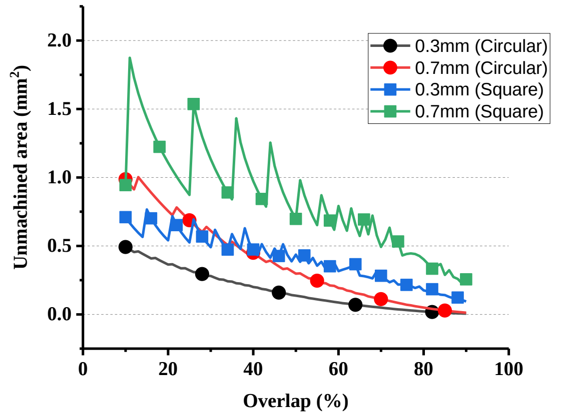


Fig. 9: Variation of the unmachined area with overlap using various size and shapes of spot

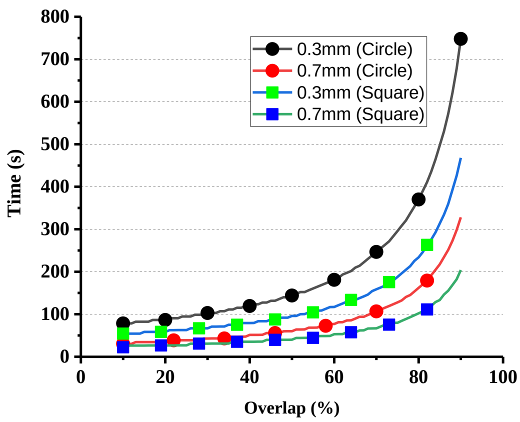


Fig. 10: Variation of machining time with overlap using various size and shapes of spot

## 4. Conclusions

We carried out an analytical study to compare the circular and square spot for machining of a circle in terms of machining time and unmachined area. From the analytical solution, we found that for the given spot size and overlap, the square spot gives minimum '$T_m$' compared to the circular spot for the same machining length. Whereas for better minimum quality i.e. minimum '$A_n$' circular spot is better than the square spot. However, the circular spot gives better machining quality in minimum 'Tm' than the square spot for different spot size. This study could be useful in industrial-scale manufacturing of various products which alongwith the high productivity rate requires better feature quality such as fabrication of metamaterial microwave absorbers using excimer laser micromachining. Furthermore, since this study does not require any additional apparatus in the manufacturing unit, it can be directly applied in the manufacturing process without adding any adding any cost.

## References


.

[1] Stratakis E, Ranella A, Farsari M, Fotakis C. Laser-based micro/nanoengineering for biological applications. Prog Quantum Electron 2009;33:127–63. doi:10.1016/j.pquantelec.2009.06.001.

[2] Piticescu R, Vlaicu I, Katz-Demyanetz A, Popov V V., Kovalevsky A, Safranchik D, et al. Powder-bed additive manufacturing for aerospace application: Techniques, metallic and metal/ceramic composite materials and trends. Manuf Rev 2019;6. doi:10.1051/mfreview/2019003.

[3] Sheokand H, Ghosh S, Singh G, Saikia M, Srivastava KV, Ramkumar J, et al. Transparent broadband metamaterial absorber based on resistive films. J Appl Phys 2017;122:105105.

[4] Rizvi NH. Production of novel 3D microstructures using excimer laser mask projection techniques. Des Test, Microfabr MEMS MOEMS 1999;3680:546. doi:10.1117/12.341245.

[5] Tien CH, Chien YE, Chiu Y, Shieh HPD. Microlens array fabricated by excimer laser micromachining with gray-tone photolithography. Japanese J Appl Physics, Part 1 Regul Pap Short Notes Rev Pap 2003;42:1280–3. doi:10.1143/jjap.42.1280.

[6] Zimmer K, Braun A, Bigl F. Combination of different processing methods for the fabrication of 3D polymer structures by excimer laser machining. Appl Surf Sci 2000. doi:10.1016/S0169-4332(99)00423-7.

[7] Lee YC, Chen CM, Wu CY. A new excimer laser micromachining method for axially symmetric 3D microstructures with continuous surface profiles. Sensors Actuators, A Phys 2005. doi:10.1016/j.sna.2004.06.006.

[8] Akhtar SN, Sharma S, Ramkumar J. Fabrication of Micro Lens Array by Excimer Laser Micromachining 2015:201–20. doi:10.1007/978-81-322-2352-8_12.

[9] Akhtar SN. Micromachining of thin films and surfaces of metals and polymers using excimer laser. Indian Institute of Technology kanpur, 2015.

[10] Singh G, Sheokand H, Ghosh S, Srivastava KV, Ramkumar J, Ramakrishna SA. Excimer laser micromachining of indium tin oxide for fabrication of optically transparent metamaterial absorbers. Appl Phys A 2019;125:23. doi:10.1007/s00339-018-2013-7.